Crystal Structures and Packing of the Tricarbonylbis(phosphine)iron(0) Complexes *trans*-Fe(CO)₃L₂ (L = PPh₂Me, PPh₃). Interplay between Arene−Arene Interactions and Phosphine Conformations

Rainer Glaser,* Paul E. Haney, and Charles L. Barnes[1a]

Department of Chemistry, University of Missouri−Columbia, Columbia, Missouri 65211

Structural effects of the nature of the phosphines on *trans*-tricarbonylbis(phosphine)iron(0) complexes *trans*-Fe-(CO)₃L₂ (L = PPh₂Me, PPh₃) are explored. The X-ray crystal structure of *trans*-Fe(CO)₃(PPh₂Me)₂, **1**, is reported. Complex **1** crystallizes in the monoclinic space group $P2_1/c$ with cell parameters $a = 15.551(6)$ Å, $b = 9.7024(12)$ Å, $c = 17.320(6)$ Å, $\beta = 91.081(11)$, and $Z = 4$. Refinement resulted in $R = 0.045$ and $R_w = 0.054$ for 3614 independent reflections with $I > 2.0\sigma(I)$. The structure of **1** is compared to *trans*-Fe(CO)₃(PPh₃)₂, **2**, and its etherate **2**·OEt₂, **3**. Further comparisons are made to the isoelectronic complex *trans*-[Co(CO)₃(PPh₃)₂]⁺, **4**, and the radical cation [Fe(CO)₃(PPh₃)₂]⁺, **2**⁺. Phosphine replacement affects intrinsic structural properties of **1**−**3** only marginally. In particular, the average Fe−P bond lengths in **1** (2.206 Å), **2** (2.217 Å), and **3** (2.216 Å) all are essentially the same in light of the standard deviations. The structures of the free and complexed phosphines also are essentially identical. Complexes **1**−**3** show a common motif of distortion from the trigonal planar (pseudo) C_{3v} bipyramid (P−Fe−P nonlinearity, Fe(CO)₃ C_{2v}-distortion, and phosphine nonequivalence). Ab initio calculations for *trans*-Fe(CO)₃(PH₃)₂ at the MP2/LANL1DZ level suggest that these distortions are due to packing. The phosphines are more or less staggered with respect to the carbonyls and the methyl groups are *gauche*. Co(I) *versus* Fe(0) replacement retains the trigonal bipyramidal structure while the oxidation of **2** to **2**⁺ yields the square pyramidal structure with longer *trans* Fe−P bonds (2.282 Å). Of special interest are the unexpected phosphine conformations in **1**−**3** and they are shown to be beneficial for the optimization of intermolecular arene−arene interactions. The crystal packing of **1** reveals displaced face-to-face and displaced T-shape arene−arene contacts that place the two phenyl rings in relative orientations that lead to stabilization in the respective benzene dimers. A rotated displaced T-shape arrangement plays a crucial role in **2**. The analyses emphasize the interplay between intermolecular arene−arene packing interactions and the phosphine conformations.

Introduction

Transition-metal organometallic reagents are becoming increasingly important in organic syntheses[2] and the many synthetic applications of iron complexes have recently been reviewed.[3] Bis(phosphine)iron carbonyl complexes such as Fe-(CO)₃(PR₃)₂ are important substrates for the formation of organoiron complexes[4] and they are especially pertinent, for example, for the production of tricarbonyl(diene) iron derivatives[5] and in olefin hydrosilation.[6] Our interest in bis(phosphine)iron carbonyl complexes originated with our studies of the equatorial carbonyl substitution by diazonium ions leading to iron−diazo complexes.[7] Electron density analyses led us to propose a new bonding model for diazonium ions[8] which was

extensively tested with theoretical[9] and experimental methods.[10,11] To properly understand the electronic relaxation
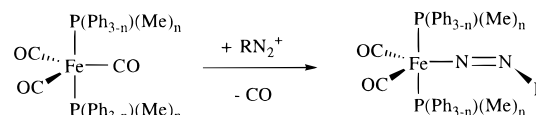
of the diazonium ions due to complexation, the structures of the complex and its precursors must be known. Since the structure of the Fe(CO)₂(N₂C₆H₅)(PPh₃)₂BF₄ salt[12] was reported,[13] we selected to investigate first the consequences of RN₂⁺/CO substitution in *trans*-Fe(CO)₃(PPh₃)₂ and to study variations of the iron(0) substrate subsequently. With this article, we begin to report on our studies of the effects of the nature of the phosphine on the exchange reaction. The crystal structure of *trans*-Fe(CO)₃(PPh₂Me)₂ (**1**) is reported and ana-

---

⊗ Abstract published in *Advance ACS Abstracts,* March 15, 1996.

(1) (a) Crystallography. (b) Part 2. Transition Metal Complexes of Diazonium Ions. For part 1, see ref 14.

(2) Colquhoun, H. M.; Horton, J.; Thompson, D. J.; Twigg, M. V. *New Pathways for Organic Synthesis: Practical Applications of Transition Metals;* Plenum Press: New York 1984.

(3) Fatiadi, A. J. *J. Res. Natl. Inst. Stand. Technol.* **1991**, *96*, 1−113.

(4) (a) Carroll, W. E.; Lalor, F. J. *J. Chem. Soc., Dalton Trans.* **1973**, 1754−1757. (b) Therien, M. J.; Ni, C. L.; Anson, F. C.; Osteryoung, J. G.; Trogler, W. C. *J. Am. Chem. Soc.* **1986**, *108*, 4037−4042 and references therein.

(5) (a) Howell, A. S.; Johnson, F. G.; Josty, P. L.; Lewis, J. *J. Organomet. Chem.* **1972**, *39*, 329−333. (b) Brookhart, M.; Nelson, G. O. *J. Organomet. Chem.* **1979**, *164*, 193−202.

(6) (a) Sanner, R. D.; Austin, R. G.; Wrighton, M. S.; Honnick, W. D.; Pittman, C. U. *Inorg. Chem.* **1979**, *18*, 928−932. (b) Liu, D. K.; Brinkley, C. G.; Wrighton, M. S. *Organometallics* **1984**, *3*, 1449−1457. (c) Liu, D. K.; Wrighton, M. S.; McKay, D. R.; Maciel, G. R. *Inorg. Chem.* **1984**, *23*, 212−220.

(7) Sutton, D. *Chem. Rev.* **1993**, *93*, 995−1022.

(8) (a) Glaser, R. *J. Phys. Chem.* **1989**, *93*, 7993−8003. (b) Glaser, R.; Choy, G. S. C.; Hall, M. K. *J. Am. Chem. Soc.* **1991**, *113*, 1109−1120. (c) Glaser, R.; Choy, G. S. C. *J. Am. Chem. Soc.* **1993**, *115*, 2340−2347.

(9) (a) Glaser, R.; Horan, C. J.; Nelson, E.; Hall, M. K. *J. Org. Chem.* **1992**, *57*, 215−228. (b) Glaser, R.; Horan, C. J. *Can. J. Chem.*, in press.

(10) (a) Horan, C. J.; Barnes, C. L.; Glaser, R. *Chem. Ber.* **1993**, *126*, 243−249. (b) Horan, C. J.; Barnes, C. L.; Glaser, R. *Acta Crystallogr.* **1993**, *C49*, 507−509. (c) Horan, C. J.; Haney, P. E.; Barnes, C. L.; Glaser, R. *Acta Crystallogr.* **1993**, *C49*, 1525−1528.

(11) (a) Glaser, R.; Chen, G. S.; Barnes, C. L. *Angew. Chem., Int. Ed. Engl.* **1992**, *31*, 740−743. (b) Chen, G. S.; Glaser, R.; Barnes, C. L. *J. Chem. Soc., Chem. Commun.* **1993**, 1530−1532.

(12) Fisher, D. R.; Sutton, D. *Can. J. Chem.* **1973**, *51*, 1697−1703.

(13) Haymore, B. L.; Ibers, J. A. *Inorg. Chem.* **1975**, *14*, 1369−1376.

lyzed in comparison to the structures of *trans*-tricarbonylbis-(triphenylphosphine)iron(0) (**2**), previously reported by us,[14] and its etherate *trans*-Fe(CO)$_3$(PPh$_3$)$_2$·OEt$_2$ (**3**) reported by Godfrey et al.[15] Comparisons also are made to the 17-electron radical cation [Fe(CO)$_3$(PPh$_3$)$_2$]$^{•+}$ (**2$^{•+}$**) and the closed-shell cation [Co-(CO)$_3$(PPh$_3$)$_2$]$^+$ (**4**) reported by Fortier, Baird, Ziegler, et al.[16] The effects of the nature of the phosphine ligand on the structures of the complexes are explored. The analysis of the conformational properties of the phosphines suggests that the optimization of intermolecular arene−arene interactions might be pertinent to the understanding of the crystal packing.

The significance of studies of the properties and reactions of iron(0) phosphine complexes in the context of studies of N$_2$ fixation has been emphasized by Hidai and Mizobe[17] since the recent structure determination of nitrogenase[18] strongly suggests iron as the active site. Leigh et al.[19] provided evidence that iron(0) complexes such as [Fe(N$_2$)(dmpe)$_2$] can mediate the conversion of coordinated N$_2$ to ammonia. The protonation of N$_\beta$ presumably is the first step in this reduction and this step competes with protonation at the metal center and N$_2$ libera-tion.[20] For example, protonation of [Fe(N$_2$)(depe)$_2$] does not yield ammonia but promotes N$_2$ loss.[21] The studies of the above exchange reactions as a function of the phosphine ligand might help to understand these observations and lead to more effective models.

Experimental Methods

Preparations of *trans*-Fe(CO)$_3$(PR$_{3-n}$R$'_n$)$_2$. Simple substitution of Fe(CO)$_5$ by phosphines produces mixtures of mono- and disubstituted complexes. While the selective syntheses of monosubstituted iron carbonyl phosphines (LFe(CO)$_4$; L = PR$_3$) can be accomplished with various catalysts,[22] the selective synthesis of disubstituted phosphine complexes presented a greater challenge. Keiter et al. achieved a one-step formation of *trans*-Fe(CO)$_3$(PR$_3$)$_2$ without the formation of Fe(CO)$_4$PR$_3$ and in the absence of the *cis*-isomer. This reaction involves refluxing Fe(CO)$_5$ and PR$_3$ in *n*-butanol with NaBH$_4$[23] or NaOH[24] and provides an improvement of Siegl's method of reducing Fe(CO)$_5$ with LiAlH$_4$ or NaBH$_4$ in refluxing THF.[25] We employed Keiter's method using NaOH.

Crystal Preparation of *trans*-Fe(CO)$_3$(PPh$_2$Me)$_2$ (1) and Data Acquisition. Single crystals of **1** were grown from acetone. A pale yellow crystal of dimensions 0.20 × 0.20 × 0.35 mm was selected for X-ray diffraction. Data were collected on a Nonius diffractometer. The cell dimensions were obtained from 25 reflections with the range 20°

(14) Glaser, R.; Yoo, Y. H.; Chen, G. S.; Barnes, C. L. *Organometallics* **1994**, *13*, 2578−2586.
(15) Lane, H. P.; Godfrey, S. M.; McAuliffe, C. A.; Pritchard, R. G. *J. Chem. Soc., Dalton Trans.* **1994**, 3249−3256.
(16) MacNeil, J. H.; Chiverton, A. C.; Fortier, S.; Baird, M. C.; Hynes, R. C.; Williams, A. J.; Preston, K. F.; Ziegler, T. *J. Am. Chem. Soc.* **1991**, *113*, 9834−9842.
(17) Hidai, M.; Mizobe, Y. *Chem. Rev.* **1995**, *95*, 1115−1133.
(18) Kim, J.; Rees, D. C. *Science* **1992**, *257*, 1677−1682.
(19) (a) Leigh, G. J.; Jimenez-Tenorio, M. *J. Am. Chem. Soc.* **1991**, *113*, 5862−5863. (b) Hills, A.; Hughes, D. L.; Jimenez-Tenorio, M.; Leigh, G. J. *J. Chem. Soc., Dalton Trans.* **1993**, 3041−3049.
(20) Yamamoto, A.; Miura, Y.; Ito, T.; Chen, H.-L.; Iri, K.; Ozawea, F.; Miki, K.; Sei, T.; Tanaka, N.; Kasai, N. *Organometallics* **1983**, *2*, 1429−1436.
(21) Komiya, S.; Akita, M.; Yoza, A.; Kasuga, N.; Fukuoka, A.; Kai, Y. *J. Chem. Soc., Chem. Commun.* **1993**, 787−788.
(22) (a) Albers, M. O.; Coville, N. J.; Ashworth, T. V.; Singleton, E. *J. Organomet. Chem.* **1981**, *217*, 385−390. (b) Butts, S. B.; Shriver, D. F. *J. Organomet. Chem.* **1979**, *169*, 191−197. (c) Conder, H. L.; Darensbourg, M. Y. *J. Organomet. Chem.* **1974**, *67*, 93−97. (d) Siegl, W. O. *J. Organomet. Chem.* **1975**, *92*, 321−328.
(23) Keiter, R. L.; Keiter, E. A.; Hecker, K. H.; Boecker, C. A. *Organometallics* **1988**, *7*, 2466−2469.
(24) Keiter, R. L.; Keiter, E. A.; Boecker, C. A.; Miller, D. R. *Synth. React. Inorg. Met.-Org. Chem.* **1991**, *21*, 473−478.
(25) See also: Brunet, J. J.; Kindela, F. B.; Neibecker, D. *J. Organomet. Chem.* **1989**, *368*, 209−212.

Table 1. Crystallographic Data for *trans*-Fe(CO)$_3$(PPh$_2$Me)$_2$ (**1**)

C$_{29}$H$_{26}$O$_3$P$_2$Fe	space group: P 2$_1$/c
$a = 15.551(6)$ Å	$T = 20$ °C
$b = 9.7024(12)$ Å	$\lambda = 0.709\ 30$ Å
$c = 17.320(6)$ Å	$\rho_{calc} = 1.374$ g cm^{-3}
$\beta = 91.081(11)°$	$\mu = 7.2$ cm^{-1}
V of unit cell = 2612.8(14) Å^3	$R = 0.045^a$
$Z = 4$	$R_w = 0.054^a$
fw = 540.31	

^{a} $R = \Sigma(||F_o| - |F_c||)/\Sigma|F_o|$ and $R_w = [\Sigma w(|F_o| - |F_c|)^2)/(w|F_o|^2)]^{1/2}$.
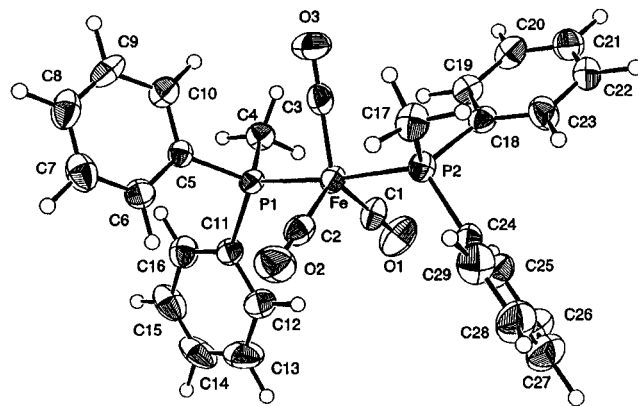
Figure 1. Perspective view of *trans*-Fe(CO)$_3$(PPh$_2$Me)$_2$ with numbering scheme. Thermal ellipsoids are drawn at the 30% probability level.
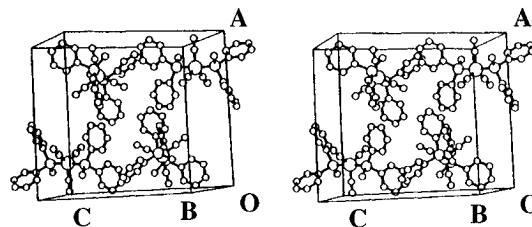
Figure 2. Stereoview of the packing interactions in *trans*-Fe(CO)$_3$-(PPh$_2$Me)$_2$.

$\leq \theta \leq 30°$. Important parameters are listed in Table 1. A total of 3760 reflections were collected with 3614 being independent, $I > 2.0\sigma$-(I), with residuals $R = 0.045$ and $R_w = 0.054$. Absorption corrections were made using the Ψ scan mode ($T_{min} = 0.91$, $T_{max} = 1.00$).

Results and Discussion

Crystal Structure of *trans*-Fe(CO)$_3$(PPh$_2$Me)$_2$ (1). An ORTEPII[26] drawing of **1** with numbering scheme and a stereo PLUTO[27] molecular packing diagram are shown in Figures 1 and 2. Structural parameters of **1** are given in Table 2 and selected average values of pertinent structural parameters of **1−4** are presented in Table 3.

The structure of **1** is a distorted trigonal bipyramid with nonequivalent phosphines. The Fe−P bond distances average 2.206 ± 0.003 Å. These bond lengths have to be considered identical because the deviations from this average are only twice as large as the standard deviations of the Fe−P bond lengths—d(Fe−P1) = 2.2029(14) Å, d(Fe−P2) = 2.2089(14). The P1−Fe−P2 backbone deviates significantly from linearity with an angle of 174.0°. The distortion is best described as a translation of the P atoms in the plane of the C2, Fe, and both P atoms such that the C2−Fe−P angles increase.

The Fe(CO)$_3$ fragment deviates from perfect trigonal planar geometry. Two of the C−Fe−C angles are almost identical

(26) Johnson, C. K. *ORTEPII*; Report ORNL-5138; Oak Ridge National Laboratory: Oak Ridge, TN, 1976.
(27) Motherwell, W. D. S. PLUTO. Program for plotting crystal and molecular structures. University of Cambridge, England, 1976.

Table 2. Selected Bond Lengths (Å), Angles (deg), and Torsion Angles (deg) of **1**

Fe−P1	2.2029(14)		P1−C11	1.826(5)
Fe−P2	2.2089(14)		P2−C17	1.827(5)
Fe−C1	1.765(6)		P2−C18	1.836(5)
Fe−C2	1.774(6)		P2−C24	1.835(5)
Fe−C3	1.756(6)		O1−C1	1.155(7)
P1−C4	1.822(5)		O2−C2	1.151(7)
P1−C5	1.816(5)		O3−C3	1.157(7)

P1−Fe−P2	173.95(6)		C6−C7−C8	120.1(5)
P1−Fe−C1	89.92(17)		C7−C8−C9	119.3(5)
P1−Fe−C2	93.03(16)		C8−C9−C10	121.7(5)
P1−Fe−C3	87.19(16)		C5−C10−C9	119.6(5)
P2−Fe−C1	90.38(17)		P1−C11−C12	121.2(4)
P2−Fe−C2	92.20(16)		P1−C11−C16	119.5(4)
P2−Fe−C3	87.73(16)		C12−C11−C16	119.3(5)
C1−Fe−C2	117.34(24)		C11−C12−C13	120.5(5)
C1−Fe−C3	125.66(24)		C12−C13−C14	119.4(6)
C2−Fe−C3	117.00(24)		C13−C14−C15	120.9(5)
Fe−P1−C4	113.02(17)		C14−C15−C16	119.7(6)
Fe−P1−C5	115.52(15)		C11−C16−C15	120.2(5)
Fe−P1−C11	118.52(16)		P2−C18−C19	121.0(4)
C4−P1−C5	102.97(22)		P2−C18−C23	119.4(4)
C4−P1−C11	102.05(22)		C19−C18−C23	119.5(5)
C5−P1−C11	102.71(21)		C18−C19−C20	120.2(5)
Fe−P2−C17	112.64(18)		C19−C20−C21	119.6(5)
Fe−P2−C18	117.03(16)		C20−C21−C22	120.6(5)
Fe−P2−C24	118.34(17)		C21−C22−C23	119.6(5)
C17−P2−C18	101.67(23)		C18−C23−C22	120.4(5)
C17−P2−C24	103.32(24)		P2−C24−C25	118.3(4)
C18−P2−C24	101.60(22)		P2−C24−C29	122.0(4)
Fe−C1−O1	178.3(5)		C25−C24−C29	119.7(5)
Fe−C2−O2	178.4(4)		C24−C25−C26	120.3(5)
Fe−C3−O3	178.8(5)		C25−C26−C27	120.8(6)
P1−C5−C6	120.5(4)		C26−C27−C28	119.2(5)
P1−C5−C10	121.5(4)		C27−C28−C29	120.4(6)
C6−C5−C10	118.0(4)		C24−C29−C28	119.7(6)
C5−C6−C7	121.1(5)			

Fe−P1−C5−C6	−89.2(5)		Fe−P1−C5−C10	89.3(5)
Fe−P1−C11−C12	1.5(4)		Fe−P1−C11−C16	−177.1(7)
Fe−P2−C18−C19	7.5(4)		Fe−P2−C18−C23	−174.8(7)
Fe−P2−C24−C25	72.7(5)		Fe−P2−C24−C29	−108.0(6)

(117.0 and 117.3° for C2−Fe−C3 and C2−Fe−C1) while the C1−Fe−C3 angle is much larger (125.7°). These distortions leave the fragment essentially planar, the sum of the C−Fe−C angles is 360.0°, and the Fe(CO)$_3$ fragment approximates C_{2v} symmetry about the Fe−C2 bond. The bond lengths and angles in the FeCO units are normal (Table 3).

In Figure 3, the molecule on the left is oriented such that the P1−Fe−P2 backbone and C2 are in the plane of the paper and the Newman projection along the direction indicated by the arrow is drawn on the right. In Figure 3, we omitted the R groups on the phosphines to clearly present the conformation about the P−Fe−P backbone. The phosphines are in a nearly perfectly staggered arrangement with respect to the carbonyls. The methyl groups at P1 and P2 are not *cis* but *gauche* in relation to one another, that is, the methyl groups avoid being eclipsed. The methyl group (C4) at P1 falls between the two carbonyls that enclose the largest angle with Fe (125.7°).

Backbone Nonlinearity, Fe(CO)$_3$ C_{2v} Distortion, and Phosphine Nonequivalence. The parameters that characterize the P−Fe−P nonlinearity and the Fe−P bonds are very similar for **1**−**3** (Table 3). While all ∠(P1−Fe−P2) angles deviate significantly from 180°, the Fe−P bond lengths of **2** (2.2201-(9), 2.2144(9)Å) and **3** (2.225(3), 2.207(3)Å) show only rather small deviations from the respective averages and the average values hardly differ at all. The average Fe−P bond distance of **1** (2.206 Å) is 0.01 Å shorter compared to those in **2** and **3** but the difference is of the same magnitude as three standard deviations, and hence, all Fe−P bonds must be considered as

Table 3. Comparison of Major Structural Parameters of **1**−**3** and Related Systems

parameter	1	2	3	4	2$^+$	53 Fe−PPh$_3$	FRTM−PPh$_3$	879 M−PMe$_3$	est FePMePh$_2$	free PPh$_3$
av Fe−P, r	2.2059(14) ± 0.003	2.2173(9) ± 0.0029	2.216(3) ± 0.009	2.240(5) ± 0.001	2.283(4) ± 0.001	2.238(36)	2.23−2.48			
∠(P1−Fe−P2)	174.0	172.6	172.5	176.5	163.4(1)					
av Fe−C	1.765(6) ± 0.009	1.770(4) ± 0.006	1.772(8) ± 0.017	1.78(1) ± 0.03	1.80(1) ± 0.01					
av C−O	1.154(7) ± 0.003	1.140(5) ± 0.015	1.148(7) ± 0.012	1.15(1) ± 0.02	1.13(1) ± 0.01					
av P−C$_{Ar}$, d	1.827(5) ± 0.009	1.832(3) ± 0.011	1.830 ± 0.006	1.807(9) ± 0.015	1.80(1) ± 0.02	1.834(9)	1.822−1.841	1.822(20)	1.83	1.831
av P1−C$_{Ar}$	1.821(5)	1.835(3)	1.834	1.807(9)	1.81(1)					
av P2−C$_{Ar}$	1.836(5)	1.829(3)	1.825	1.808(9)	1.82(1)					
av Fe−C−O	178.5(5) ± 0.3	179.2(3) ± 0.2	179.1 ± 0.7	178.5(9) ± 1.2	178(1) ± 1					
av C−P−C, β	102.39(23) ± 1	102.52(16) ± 2.3	102.9 ± 1.6			102.928(883)	101.9−106.1	101.212(229)	102.3	102.8
av Fe−P−C, α	115.85	115.77	115.48			115.403(739)	112.6−116.2			
Σ∠(C−Fe−C)	360.0	360.0	359.9							
Σ∠(C−P1−C)	307.7	307.6	309.5							
Σ∠(C−P2−C)	306.6	307.5	307.7							
Σ∠(M−P1−C)	347.1	347.3	345.7							
Σ∠(M−P2−C)	348.0	347.3	347.2							

^{a} Distances in Å and angles in degrees. ^{b} FRTM = first-row transition metal. ^{c} Data for **2**$^+$ and [Co(CO)$_3$(PPh$_3$)$_3$]$^+$ from ref 16. Data in columns 7−10 from ref 44.
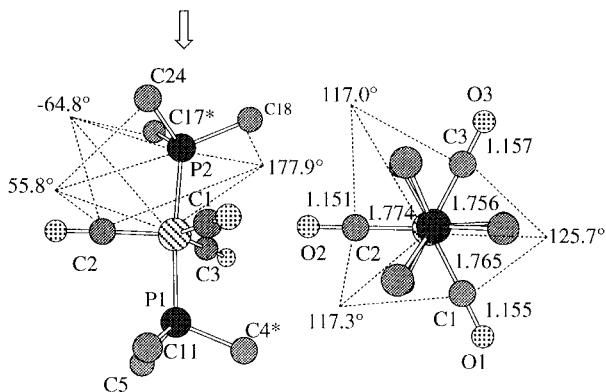
Figure 3. Newman projection of the solid state structure of *trans*-Fe-(CO)$_3$(PPh$_2$Me)$_2$ along the direction indicated by the arrow illustrates the conformations about the P–Fe–P bonds. The phosphine substituents are omitted for clarity. The methyl carbon atoms are marked by an asterisk.

Table 4. Energy Requirements For Distortions in *trans*-Fe(CO)$_3$(PH$_3$)$_2$[a]

| entry	Fe–P1	Fe–P2	α	β	E_{tot}	E_{rel}
1[b]	2.179	2.179	90	120	−376.623 253	
2	2.199	2.159	90	120	−376.623 083	0.11
3	2.179	2.179	95	120	−376.615 832	4.66
4	2.179	2.179	90	115	−376.622 312	0.59
5	2.179	2.179	95	115	−376.620 473	1.74

[a] MP2/LANL1DZ level. Bond lengths in Å and angles in degrees. Total energies (E_{tot}) in atomic units and relative energies (E_{rel}) in kcal/mol. [b] Optimized D_{3h} symmetric minimum. See ref 14 for details.

essentially identical. Consequently, it is no surprise that the structures of the phosphines hardly differ as far as the "hard" parameters are concerned; the sums of the angles ∠(C–P–C) and ∠(M–P–C) involving P1 or P2, respectively, and the average P1–C$_{Ar}$ or P2–C$_{Ar}$ bond lengths are very similar. The only significant nonequivalence between the two coordinated phosphines therefore relates to their conformations (*vide infra*).

The structural differences in the Fe(CO)$_3$ units due to the choice of PPh$_3$ or PPh$_2$Me are very small. Compared to **2** and **3**, the average Fe–C and C–O bond distances in **1** are somewhat shorter and longer, respectively, but these differences are within standard deviations and the variations between individual Fe–C and C–O bonds within a given complex can be larger in magnitude. The Fe(CO)$_3$ fragments in **2** and **3** are not perfectly trigonal but almost planar (see Σ ∠(C–Fe–C) in Table 3). In both cases and as with **1**, two of the C–Fe–C angles are essentially equivalent (118.1 and 118.3° for **2**; 117.1 and 116.9° for **3**) while the other is appreciably larger (123.6° for **2**; 125.9° for **3**).

Based on the reoccurrence of the common structural motif in **1**–**3**—nonlinear P–Fe–P backbone, C_{2v}-distorted Fe(CO)$_3$ fragments, and phosphine nonequivalence—one might be inclined to consider this motif intrinsic and the features significant.
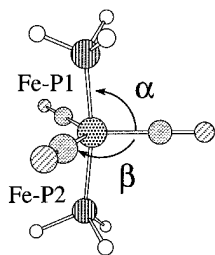
However, we have shown previously in a higher level ab initio study that *trans*-Fe(CO)$_3$(PH$_3$)$_2$ does prefer D_{3h} symmetry in the gas phase. This theoretical result would suggest that it is not a common intrinsic feature but that it is the packing that causes the common types of distortions. We have now carried out a series of calculations for *trans*-Fe(CO)$_3$(PH$_3$)$_2$ to explore the energetic costs associated with distortions of the types observed in the solid state structures. All calculations were carried out at the MP2/LANL1DZ level as described previously[14] and the results are summarized in Table 4. We have examined the consequences of (a) different Fe–P bond lengths by shortening and lengthening, respectively, of one Fe–P bond by 0.02 Å (entry 2), of (b) distortions of the P–Fe–P backbone

in the direction found in the solid state (entry 3, α variation), of (c) Fe(CO)$_3$ fragment C_{2v}-distortions (entry 4, β variation), and of (d) a combination of the latter two (entry 5, α and β variations). In each case, we modeled distortions that slightly exceed the magnitude of the distortions found in the crystals of **1**–**3**. We find that an asymmetric distortion of the Fe–P bond lengths, even when exaggerated, affects the energy of the complex very little. On the other hand, even small deformations of the P–Fe–P backbone (α variation) require significant energy. Most importantly, entries 3–5 demonstrate that deformations of the P–Fe–P backbone require *much less energy when the α-increase is accompanied by β-reduction*. These results strongly suggest a correlation between the P–Fe–P backbone nonlinearity and the C_{2v}-distortion of the Fe(CO)$_3$ fragment. In the solid state, endothermic internal distortions of this type must be overcompensated by intermolecular interactions, and the phosphine nonequivalence provides a clue as to the nature of these intermolecular interactions.

Conformations of Complexed Phosphines. Dunitz[28] described triphenylphosphines as propellers because the phenyl groups are tilted in the same direction. The conformational patterns found in **1**–**3** are more complicated. The tilt angles at the P atom are in the same direction for the PPh$_3$ compounds **2** and **3**. We described previously for **2** that two phenyl groups at P1 are characterized by tilt angles of about 30° (28.1, 28.3°) and a third much higher tilt of more than 60° (61.5°). The phenyl groups at P2 are twisted in the opposite direction and in a complementary fashion; two tilt angles of about −60° (−54.6, −56.7°) and one that is −30.4°. In **3**, the phenyl groups of one phosphine ligand are just as in the case of the P1 phosphine in **2** in that two tilt angles are about 30° (32.3, 28.2°) and one is close to 60° (59.3°). The tilt angles at the other phosphine are all about 40° (37.3, 43.5, 40.2°) and are oriented in a common direction. Obviously, the phosphine conformations reflect and, in fact, most likely are due to packing.

The conformational preferences of the PPh$_2$Me phenyl groups of **1** are shown in Figure 4. The phenyl groups within each phosphine assume drastically different conformations. When viewed along the P–Fe–P direction, one phenyl ring is seen side-on while the other is oriented such as to expose one of its faces in the best possible fashion. The phenyl groups at P1 are perpendicular to each other with tilt angles of about 89 and 2° and the phenyl groups at P2 are twisted in a similar fashion with tilt angles of about 8 and 73°. This arrangement lends itself perfectly to optimize intermolecular phenyl–phenyl interactions. In Figure 5, we have redrawn a part of the unit cell that shows the intermolecular interactions between the two phenyl groups of one phosphine of **1** with two phenyl groups of two different molecules in neighboring positions. As can be seen, one phenyl–phenyl T-shape contact and one displaced face-to-face interaction are realized. We have described the P–C conformations in **2** previously and their relevance to crystal

(28) Bye, E.; Schweizer, B.; Dunitz, J. D. *J. Am. Chem. Soc.* **1982**, *104*, 5893–5898.
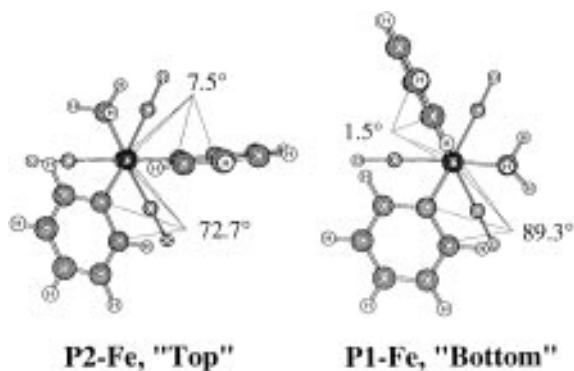
Figure 4. Newman projections of the solid state structure of *trans*-Fe(CO)$_3$(PPh$_2$Me)$_2$ along the P1–Fe and P2–Fe bonds show the conformations about the P–R bonds.
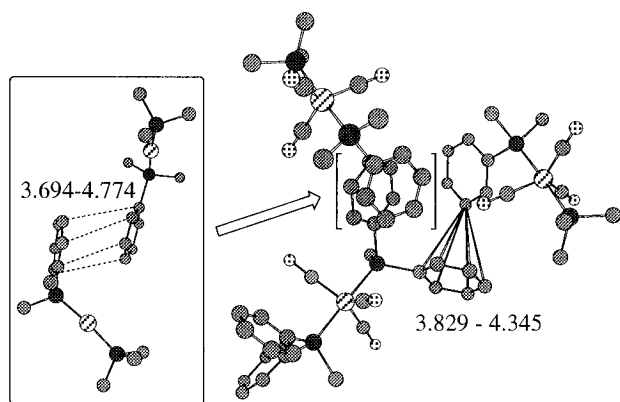

Figure 5. Intermolecular phenyl-phenyl off-center face-to-face and T-shape interactions. These appear responsible to a large degree for the phosphine conformations in **1**.
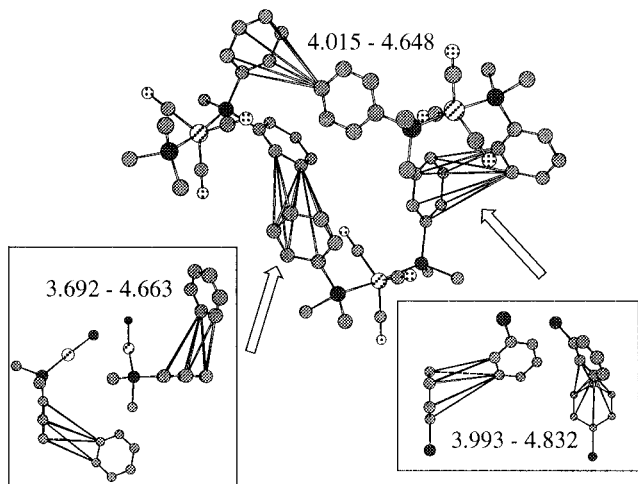
Figure 6. Intermolecular phenyl–phenyl interactions in **2**.

packing can be demonstrated with Figure 6. Aside from one T-shape contact, we find two contacts which most closely resemble the "displaced T-shape" but the H-donor molecule also is rotated to obtain the "rotated displaced T-shape" structure.

Ab initio studies of the benzene dimer (Figure 7) suggest a small intrinsic preference for the parallel displaced face-to-face benzene dimer (at 3.9 Å) over the T-shaped isomer (at 5.0 Å) and the displaced T-shaped isomer (at 4.9 Å) at their respective equilibrium distances and in agreement with spectroscopic gas phase data.[29] The rotated displaced T-shape structure does not correspond to a minimum for the benzene dimer, and its relative
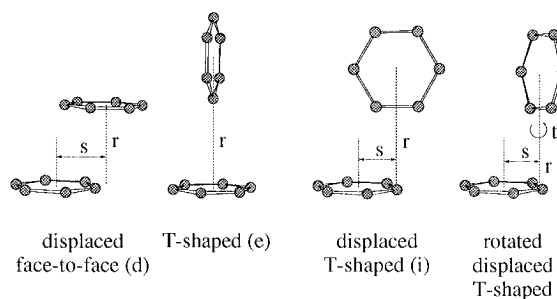
Figure 7. Schematic drawings of the displaced face-to-face, T-shape, displaced T-shape, and rotated displaced T-shape benzene dimers. The numbering given in parentheses for the first three structures refers to the article by Hobza, Selzle, and Schlag.[30]

energy is not known. The preference for these types of benzene–benzene arrangements also are found in other solids[30–32] and in solution.[33] The interactions in benzene dimer and related systems have been shown to be mostly electrostatic[34,35] and experimental studies support this view.[36] The role of intra- and intermolecular "weak polar" interactions between ligands also is being recognized.[37] While each long-range interaction is comparatively weak (<1.5 kcal/mol), the combination of several of these weak interactions can overcompensate the energy requirements discussed for the internal deformations. It is thus possible that the optimization of such arene–arene interactions in fact determines the crystal packing.

Characteristics of the PPh$_3$ and PPh$_2$Me Ligands. Tolman pioneered studies of the electronic and steric effects on structures, reactivities, and bonding of complexed phosphines with the introduction of parameters that measure electronic and steric effects of phosphines. The χ increment system was developed to quantify electronic effects of phosphines based on stretching frequencies $\nu_{CO}(A_1)$ in Ni(CO)$_3$L (L = phosphine) complexes.[38] Steric requirements of phosphines were described with their "cone angles" (θ) based on Corey–Pauling–Koltun (CPK) models.[39] The successive replacement of Ph by Me in the phosphine L leads to a linear reduction of $\nu_{CO}(A_1)$, and the substituent contributions for Ph and Me are 4.3 and 2.6 cm^{-1}. The replacement of Ph by Me groups reduces the steric bulk of the phosphine and the cone angles for PPh$_3$ and PPh$_2$Me are 145 and 136°, respectively. Tolman's analysis suggests primarily steric differences between PPh$_3$ and PPh$_2$Me.

Giering and co-workers built on Tolman's approach by inclusion of thresholds for the steric parameter (θ) and with attempts at separating Tolman's electronic parameter (ν) into

(29) Hobza, P.; Selzle, H. L.; Schlag, E. W. *Chem. Rev.* **1994**, *94*, 1767–1785.

(30) Desiraju, G. R.; Gavezzotti, A. *J. Chem. Soc., Chem. Commun.* **1989**, 621–623.

(31) (a) Petsko, G. A.; Burley, S. K. *Science* **1985**, *229*, 23–28. (b) Burley, S. K.; Petsko, G. A. *J. Am. Chem. Soc.* **1986**, *108*, 7995–8001.

(32) Chen, G. S.; Wilbur, J. K.; Barnes, C. L.; Glaser, R. *J. Chem. Soc., Perkin Trans. 2* **1995**, 2311–2317.

(33) Jorgensen, W. L.; Severance, D. L. *J. Am. Chem. Soc.* **1990**, *112*, 4768–4774.

(34) Price, S. L.; Stone, A. J. *J. Chem. Phys.* **1987**, *86*, 2859–2868.

(35) Hunter, C. A. *Angew. Chem., Int. Ed. Engl.* **1993**, *32*, 1584–1586.

(36) (a) Cozzi, F.; Annuziata, R.; Cinquini, M.; Siegel, J. S. *J. Am. Chem. Soc.* **1993**, *115*, 5330–5331. (b) Cozzi, F.; Ponzini, F.; Annuziata, R.; Cinquini, M.; Siegel, J. S. *Angew. Chem., Int. Ed. Engl.* **1995**, *34*, 1019–1020. (c) Schwabacher, A. W.; Shuhong, Z.; Davy, W. *J. Am. Chem. Soc.* **1993**, *115*, 6995–6996.

(37) See for example: (a) Karpishin, T. B.; Stack, T. D. P.; Raymond, K. N. *J. Am. Chem. Soc.* **1993**, *115*, 6115–6125. (b) Kawamoto, T.; Hammes, B. S.; Haggerty, B.; Yap, G. P. A.; Rheingold, A. L.; Borovik, A. S. Submitted for publication. We thank the authors for making the manuscript available to us prior to publication.

(38) Tolman, C. A. *J. Am. Chem. Soc.* **1970**, *92*, 2953–2956.

(39) (a) Tolman, C. A. *Chem. Rev.* **1977**, *77*, 313–348. (b) Schenkluhn, H.; Scheidt, W.; Weimann, B.; Zahres, M. *Angew. Chem., Int. Ed. Engl.* **1979**, *18*, 401–402.

σ- and π-components. The Fe−P bond lengths in a series of complexes (η^5-Cp)(CO)(L)FeCOMe (L = phosphine) vary only over a narrow range of 2.195 ± 0.015 Å, and this observation provided the basis for a discussion of thresholds for the onset of steric effects.[40] Giering et al.[41] proposed two systems for classification of metal−phosphine interactions. The phosphines were partitioned into group 1 (σ-donors) and group 2 (σ-donors/π-acceptors) ligands by correlating the terminal stretching frequencies in series of three Fe complexes—(η^5-Cp)FeL(CO)-COMe, (η^5-Cp′)FeL(CO)COMe, (η^5-Cp)FeL(CO)Me—with the reduction potentials E_L^o of the complexes. In earlier work, correlations between E_L^o and the pK_a values of HL⁺ were explored for (η^5-Cp′)MnL(CO)₂, separating phosphines into three classes: class I (σ- and π-donor) R₃P (R = Et, Bu, Cy), class II (σ-donor) Me₃P, R$_{3-n}$Ph$_n$P (n = 1,2; R = Et, Me), and (*p*-XPh)₃P (X = H, Me, OMe), and class III (σ-donor/π-acceptor) (*p*-ClPh)₃P, (RO)₃P (R = Ph, Me, Et, *i*-Pr), and Ph₂(MeO)P. According to these classification schemes, the PPh₃ and PPh₂Me ligands both are considered pure σ-donors belonging to group 1 and class II. Other classification schemes also emphasize the strong σ-donor component while still considering phosphines as weakly π-back-bonding.[42]

Tolman pointed out that "the idea of ligand cone angles should be tested experimentally whenever possible", and indeed such studies were reported.[43] Geometrical deformations of triphenylphosphines and of other PA₃ phosphines in crystal structures were studied extensively by Orpen et al.[44] More than 1800 unique Z−PC₃ units were examined and a strong negative correlation between the mean P−C distance *d* and the mean C−P−C angle *β* was established. In Table 3, we included pertinent data from this study by Orpen et al., and we provide estimates for **1** that are based on the data for the Fe−PPh₃ and Fe−PMe₃ systems and the assumption of additivity. The *d* values are 1.83 Å and the *β* angles are 102 −103° for **1**−**3** in complete agreement with Orpen's averages. Note that the *d* and *β* values equal that of the free ligand corroborating Orpen's observation that phosphines bound to transition metals located centrally in the periodic table have P−C distances and C−P−C angles that are very similar to those of free PPh₃.

Structural Effects of Single Electron Oxidation. Comparisons to [Fe(CO)₃(PPh₃)₂]⁺[PF₆]⁻·0.5CH₂Cl₂) and [Co(CO)₃(PPh₃)₂]⁺[PF₆]⁻·CH₂Cl₂. In a study by Fortier, Baird, Ziegler, et al.[16] the crystal structures were reported of the PF₆⁻ salts of the 17-electron radical cation [Fe(CO)₃(PPh₃)₂]•⁺, **2**•⁺, and of the diamagnetic cation [Co(CO)₃(PPh₃)₂]⁺, **4**, which is isoelectronic with **2**. The structure of **4** resembles **1**−**3** in that it is trigonal-bipyramidal with axial phosphines (∠(P−Fe−P) = 176.1(1)°) and an equatorial planar Co(CO)₃ unit (∠(C−Fe−C) are 117.8(4), 119.5(4), and 122.7(5)°). The Co−P bonds (2.239(5), 2.240(5) Å) are virtually identical and more than 0.02 Å longer than in **1**−**3**. The distortions common to **1**−**3** are much less pronounced in **4** and, in this context, it is important

to note that the phenyl twists in **4** do result in propeller type phosphine conformations. The iron(I) complex was found to assume a distorted square-pyramidal structure with two *trans* basal phosphines. The Fe−P bonds are 2.282(4) Å long and they are elongated very significantly—by more than 0.065 Å—compared to **1**−**3**. The bond lengths characterizing the Fe-(CO)₃ units are not well resolved for **2**•⁺ but it is clear that these bonds are hardly affected by the oxidation. Qualitative MO considerations suggest that the one-electron oxidation of *trans*-Fe(CO)₃(PH₃)₂ should distort from the trigonal-bipyramidal structure to eliminate the degeneracy of the a₁ and b₂ HOMOs. The ²A₁ state prefers the square-pyramidal **a**-structure while the ²B₂ state prefers a C_{2v} symmetric **b**-structure with one small ∠(C−Fe−C) angle. According to density functional calculations, both of these structures correspond to local minima with a modest preference for the ²A₁ state (≈5 kcal/mol).

a-structure   **b**-structure
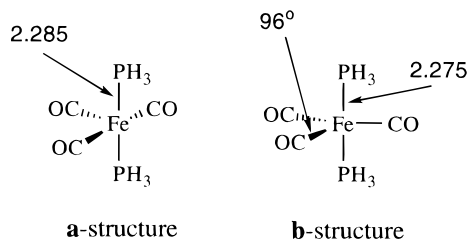
Importantly, the calculations by Ziegler, et al. show a difference between the Fe−P bonds in the **a**- and **b**-structures that is much smaller than the respective difference between **1**−**3** and the cation **2**•⁺. Only a minor part of the Fe−P elongation associated with the oxidation of **2** to **2**•⁺ is the result of Fe-(CO)₃ distortion.

Conclusion

The structural effects of the nature of the phosphine ligand on the tricarbonylbis(phosphine)iron(0) complexes *trans*-Fe-(CO)₃L₂ (L = PPh₂Me, PPh₃) were explored. The phosphines are dominantly σ-donors and differ mostly in their steric requirements as indicated by their cone angles of 145 (PPh₃) and 136° (PPh₂Me). The phosphines are more (**1**) or less (**2**, **3**) staggered with respect to the carbonyls and the methyl groups in **1** are *gauche*. The structures of the free and complexed phosphines are essentially the same in corroboration of Orpen's postulate. The average Fe−P bond lengths in **1** (2.206 Å), **2** (2.217 Å), and **3** (2.216 Å) are essentially identical, and all are at least 0.065 Å shorter than those in the radical cation **2**•⁺. The phosphine replacement has virtually no effect on the structures of the approximately C_{2v} symmetric Fe(CO)₃ units. Complexes **1**−**3** share a common structural motif—nonlinear P−Fe−P backbone, C_{2v}-distorted Fe(CO)₃ fragments, and phosphine nonequivalence—and we have argued that this structural motif, although common, is not an intrinsic feature but rather is forced by the packing. Quantum mechanical studies show that these internal distortions do not stabilize the free complex, and hence, the energy required for these distortion must be overcompensated by intermolecular interactions and the phosphine nonequivalence provides a clue as to the nature of these intermolecular interactions.

Ab initio calculations show that free *trans*-Fe(CO)₃(PH₃)₂ prefers D_{3h} symmetry and that distortions from P−Fe−P linearity and the C_{2v}-distortion of the Fe(CO)₃ fragment are correlated. The fact that similar distortions are observed for **1** and for the complexes **2** and **3** with their potentially 3-fold symmetric PPh₃ ligands corroborates our view that the distortions are due to intermolecular forces as opposed to internal effects. Furthermore, the structure of the closely related

(40) Liu, H. Y.; Eriks, K.; Prock, A.; Giering, W. P. *Organometallics* **1990**, *9*, 1758−1766.

(41) (a) Golovin, M. N.; Rahman, M. M.; Belmonte, J. E.; Giering, W. P. *Organometallics* **1985**, *4*, 1981−1991. (b) Rahman, M. M.; Liu, H. Y.; Eriks, K.; Prock, A.; Giering, W. P. *Organometallics* **1989**, 8, 1−7.

(42) (a) Fiedler, S. S.; Osborne, M. C.; Lever, A. B. P.; Pietro, W. J. *J. Am. Chem. Soc.* **1995**, *117*, 6990−6993. (b) For phosphines with exceptional π-acceptor character, see: Moloy, K. G.; Petersen, J. L. *J. Am. Chem. Soc.* **1995**, *117*, 7696−7710.

(43) See, for example: Cotton, F. A.; Darensbourg, D. J.; Klein, S.; Kolthammer, B. W. S. *Inorg. Chem.* **1982**, *21*, 2661−2666.

(44) (a) Dunne, B. J.; Morris, R. B.; Orpen, A. G. *J. Chem. Soc., Dalton Trans.* **1991**, 653−661. (b) Dunne, B. J.; Morris, R. B.; Orpen, A. G. *Acta Crystallogr.* **1991**, *C47*, 345−347.

complex **4** contains a propeller type PPh$_3$ and the distortions found in **1**−**3** essentially do not occur in **4**. Of particular interest are the unexpected phosphine conformations. In **1**, for example, the phenyl groups on each phosphine are almost perpendicular to each other. We have shown that such arrangements lend themselves very well to optimize intermolecular arene−arene interactions. The crystal packing of **1** reveals displaced face-to-face and displaced T-shape arene−arene contacts that place the two phenyl rings in relative orientations that lead to stabilization in the respective benzene dimers. In **2**, a rotated displaced T-shape arrangement also plays a crucial role. While each long-range interaction is comparatively weak, the combination of several of these weak interactions can overcompensate the energy requirements discussed for the internal deformations. It is thus entirely possible that the optimization of arene−arene interactions determines the crystal packing.

Our analyses emphasize that the phosphine conformations are likely to result from the interplay between intermolecular arene−arene interactions and that the stereochemical properties of the complexes in the solid do not necessarily reflect intrinsic features of the free complexes themselves.

Supporting Information Available: Full lists of crystallographic data atomic coordinates, positional parameters, bond lengths and angles, and anisotropic thermal parameters of **1** (5 pages). Ordering information is given on any current masthead page. The crystallographic data also were deposited at the Cambridge Crystallographic Data Centre and can be obtained from the Director, Cambridge Crystallographic Data Centre, 12 Union Road, Cambridge CB2 1EZ, UK.

IC9509894